Journal of Constructional Steel Research 90 (2013) 60–71

Contents lists available at ScienceDirect

Journal of Constructional Steel Research

A novel formulation of the flexural overstrength factor for steel beams

Esra Mete Güneyisi [a,*], Mario D'Aniello [b], Raffaele Landolfo [b], Kasım Mermerdaş [c]

[a] Department of Civil Engineering, Gaziantep University, Gaziantep, Turkey
[b] Department of Structures for Engineering and Architecture, University of Naples "Federico II", Naples, Italy
[c] Department of Civil Engineering, Hasan Kalyoncu University, Gaziantep, Turkey

ARTICLE INFO

Article history:
Received 23 January 2013
Accepted 16 July 2013
Available online 19 August 2013

Keywords:
Analytical modelling
Flexural overstrength
Experimental database
Steel beams
Steel structures

ABSTRACT

The ductile design of steel structures is directly influenced by the flexural behaviour of steel beams, which should be sufficient to allow plastic hinges to rotate until the collapse mechanism is completely developed. To guarantee the achievement of such a performance, the beam flexural overstrength must be quantified to appropriately apply capacity design principles. To this aim, analytical formulations to predict the flexural overstrength factor (s) of steel beams with a wide range of cross-section typologies (I and H sections, square and rectangular hollow sections) were developed based on gene expression programming (GEP). An experimental database was gathered from the available literature and processed to obtain the training and testing databases for the derivation of the closed-form solution through GEP. The independent variables used for the development of the prediction models were the geometric properties of the sections, the mechanical properties of the material, and the shear length of the steel beams. The predictions of the proposed GEP-based models were compared with the results obtained using the existing analytical equations proposed in the current literature. Comparative analysis revealed that the proposed formulation provides a more accurate prediction of beam overstrength.

1. Introduction

The flexural behaviour of steel beams plays a key role in the structural performance of steel moment-resisting frames. The main response parameters governing the beam behaviour are the rotation capacity and the flexural ultimate resistance [1,2]. The former is the source of the local ductility supply needed to achieve a global dissipative structural behaviour, whereas the latter governs the flexural overstrength, which must be accurately known to appropriately apply capacity design principles, as currently implemented in all modern seismic codes. This design philosophy leads to the formation of a ductile mechanism in the structures to dissipate the seismic input energy through plastic deformations within specific parts (namely, members and/or connections) of the structure itself [3]. Additionally, it may be necessary to design the main structural elements along a similar design approach under non-seismic conditions, such as in the case of robustness under exceptional loading, where it is crucial to enhance the local resistance of principal members to prevent progressive collapse [4]. Hence, both under seismic conditions and in the case of exceptional loading, it is fundamental to guarantee that the structural elements connected to ductile parts are designed to resist the maximum strength experienced by the latter. Thus, an effective estimation of the level of hardening developing in such elements prior to strength degradation is essential at the design stage for the safe application of capacity design rules [5,6].

To this end, several studies have been carried out to derive analytical formulations for the rotation capacity and flexural overstrength of the structural steel members [1,2,7–15]. In particular, some studies have used computational tools (namely, finite element analysis) or have developed computational aids. For example, in the study of Wilkinson and Hancock [15], finite element analysis was applied to cold-formed rectangular hollow section (RHS) beams to predict the rotation capacity of class 1 (plastic) and 2 (compact) beams. Gioncu et al. [9] and Anastasiadis et al. [10] developed a computer programme (DUCTROT-M) to determine both the flexural strength and the available rotation capacity of wide-flange beams.

Recently, novel approaches based on soft computing have been employed to address the analysis and design of steel structures, thus borrowing from artificial intelligence philosophies widely used to solve sophisticated engineering problems in the past [16–29]. For example, in the study of Saka [16], a genetic-algorithm-based optimum design is presented for pitched-roof steel portal frames with haunches for the rafters at the eaves. Gholizadeh et al. [17] used finite element (FE) and soft computing techniques, namely, back-propagation (BP) neural network and adaptive neuro-fuzzy inference system (ANFIS) methods, to propose models for the estimation of the critical buckling load of the web posts of castellated steel beams. Fonseca et al. [18] utilised neural networks to forecast steel beam patch load resistance, comparing the results with preceding models and existing design formulae. They concluded that the networks' percentage errors relative to the experimental results confirm the possibility of using the unified methodology to generate new data accurately. In the study of Gandomi et al. [19], an alternative approach for predicting the flexural resistance

* Corresponding author. Tel.: +90 342 3172423; fax: +90 342 3601107.
E-mail address: eguneyisi@gantep.edu.tr (E.M. Güneyisi).

0143-974X/$ – see front matter © 2013 Elsevier Ltd. All rights reserved.
http://dx.doi.org/10.1016/j.jcsr.2013.07.022

and initial rotational stiffness of semi-rigid joints in steel structures using linear genetic programming was proposed. Furthermore, in another study [20], using genetic programming, a solution for the rotation capacity of wide flange beams was illustrated based on experimental results from the literature.

The review of state of the art clearly highlighted that soft computing techniques are very promising methods providing practical and accurate prediction formulae. In particular, gene expression programming (GEP) is the most effective and versatile approach because it does not require predefined functions, unlike analytical methods. Indeed, in GEP, the functions are randomly formed, and those best fitting the experimental results are selected.

The above consideration has motivated the authors to implement GEP to develop explicit formulations of the flexural overstrength factor for steel beams with a reasonable degree of accuracy. To the best of the authors' knowledge, the current technical literature does not feature any prediction models derived from GEP for this purpose. To this end, in the present paper, two GEP-based mathematical models developed to predict the flexural overstrength factor for steel beams with I–H sections and rectangular and square hollow sections (RHS, SHS) are described and discussed. These models are derived using geometrical parameters (namely, cross-section properties) and mechanical parameters (namely, material strength and shear length) collected from a wide-ranging experimental database (covering 141 tests) available from the literature.

2. Flexural overstrength factor

2.1. Definition

The flexural overstrength factor (s) is a generally intended non-dimensional parameter measuring the ultimate bending capacity of steel beams, which can be noticeably larger than the plastic bending strength because of the strain hardening that can be experienced prior to the complete development of local buckling or fractures [1]. This factor can be given by the following ratio:

$$s = \frac{f_{LB}}{f_y} \tag{1}$$

where f_{LB} is the stress corresponding to the complete development of local buckling and f_y is the yielding stress.

However, this parameter can also be calculated using the following more practical expression:

$$s = \frac{M_{max}}{M_p} \tag{2}$$

where M_{max} represents the maximum moment that can be reached by the structure, while M_p is the theoretical full plastic moment. The definition is illustrated in the generalised force displacement curve of a member able to withstand plastic deformation shown in Fig. 1.

2.2. Flexural overstrength factor in current design codes

The consistent and reliable structural design of frames requires that the flexural overstrength factor be known. A simple definition of s was given in AISC 341-10 [21] as $1.1R_y$, where R_y is the ratio between the expected yield stress and the specified minimum yield stress. This parameter ranges from 1.1 to 1.5 depending on the steel grade and thus only accounts for the variability of material characteristics. The current Italian code NTC 2008 [22] and Eurocode 8 [23] consider a similar overstrength factor, given by $1.1\gamma_{ov}$. In particular, Eurocode 8 [23] suggests the use of $\gamma_{ov} = 1.25$, leading to an overall overstrength factor of $1.10 \times 1.25 = 1.375$. It should be taken into account that AISC 341-10 [21] evidently distinguishes the overstrength due to random material variability, the expected yield strength, strain-hardening, and other possible sources by means of the 1.1 factor, whereas this clear difference is not made in Eurocode 8, where the flexural overstrength due to strain-hardening and other sources is not mentioned [1]. Only the late Italian code OPCM 3274 [11,24] overcame this limit by providing s using the formulation suggested by Mazzolani and Piluso [24]. In accordance with that code, s can be estimated for I and H sections subjected to axial and/or flexural loads considering steel grade as follows:

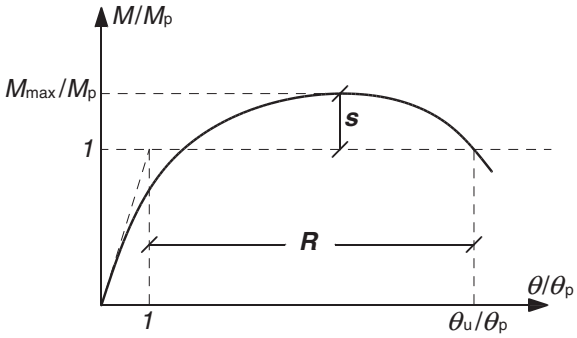

Fig. 1. Generalised moment–rotation curve for a steel beam [1].

$$s = \frac{1}{0.695 + 1.632\lambda_f^2 + 0.062\lambda_w^2 - 0.602\dfrac{b_f}{L_v}} \le \frac{f_u}{f_y} \tag{3}$$

where

$$\lambda_f = \frac{b_f}{2.t_f}\sqrt{\frac{f_y}{E}} \tag{4}$$

$$\lambda_w = \frac{d_{w,e}}{t_w}\sqrt{\frac{f_y}{E}} \tag{5}$$

are the flange and the web slenderness parameters, respectively, with b_f being the flange width, t_f the flange thickness, $d_{w,e}$ the compressed part of the web, and t_w the web thickness. Moreover, the ratio b_f/L_v accounts for the effect of the stress gradient along the member axis, with L_v being the shear length, i.e., the distance between

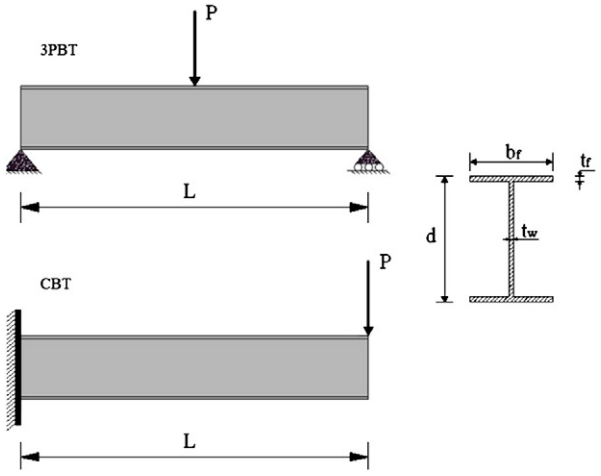

Fig. 2. Schematic views of the test arrangement and geometry of cross-section variables for I–H steel beams.

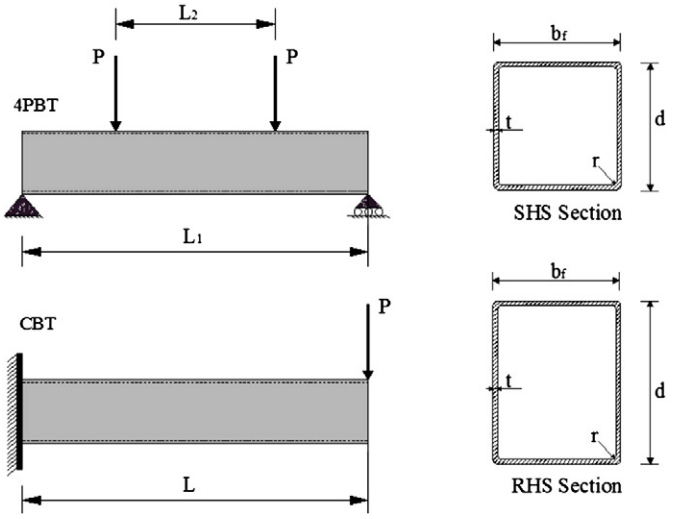

Fig. 3. Schematic views of the test arrangement and geometry of cross-section variables for RHS–SHS steel beams.

the plastic hinge and the point of zero moment. The compressed part of the web, i.e., the effective compressed web, can be computed according to [25] as

$$d_{w,e} = \frac{1}{2}\left(1 + \frac{A}{A_w}\rho\right)d_w \tag{6}$$

where A is the section area, A_w is the web area, d_w is the web depth, and ρ is the non-dimensional axial load, i.e., the ratio between the axial load and the squash load.

2.3. Review of the existing analytical formulations

2.3.1. Flexural overstrength factor for I and H profiles

To estimate the overstrength factor of the steel beams in relation to the cross-sectional dimensions and material characteristics, various relations have been proposed in the literature [1,2,11,25–27]. Kato [25,26] proposed empirical equations to estimate the flexural overstrength based on the results of 68 tests conducted on "stub-column" specimens with different steel grades and local (flange and web) slenderness parameters. The normalised overstrength s was obtained by multiple regression analysis as function of the flange and web slenderness for each grade of steel, whose expression is given by the following:

$$\frac{1}{s} = 0.6003 + \frac{1.600}{\alpha_f} + \frac{0.1535}{\alpha_w} \tag{7}$$

where

$$\alpha_f = \frac{E}{f_y}\left(\frac{t_f}{b_f/2}\right)^2 \tag{8}$$

is the slenderness parameter of the flange and

$$\alpha_w = \frac{E}{f_y}\left(\frac{t_w}{d_w}\right)^2 \tag{9}$$

is the slenderness parameter of the web, d_w is the web height, t_w is the web thickness, f_y is the yield strength, and E is the modulus of elasticity of steel.

Brescia [2] proposed a novel expression of s, recalibrating the coefficients of the formulation developed by [24] and adopted by OPCM 3274 [11,24]. From the multiple regression of a limited set of experimental data, she derived the following expression:

$$\frac{1}{s} = 0.349 + 0.827\lambda_f^2 + 0.03\lambda_w^2 - 0.239\frac{b_f}{L_v} - 0.045\frac{E}{E_h} + 0.263\frac{\varepsilon_h}{\varepsilon_y}. \tag{10}$$

Moreover, considering the average mechanical properties of European mild carbon steel, Eq. (10) can be specialised as follows [2]:

$$\frac{1}{s} = 1.323 + 0.827\lambda_f^2 + 0.03\lambda_w^2 - 0.239\frac{b_f}{L_v} \tag{11}$$

More recently, in a study by D'Aniello et al. [1], another empirical equation for predicting s was derived by multiple linear regression analysis using a wider database of experimental tests, as follows:

$$\frac{1}{s} = 1.71 + 0.167\lambda_f^2 + 0.006\lambda_w^2 - 0.134\frac{b_f}{L_v} - 0.007\frac{E}{E_h} - 0.0053\frac{\varepsilon_h}{\varepsilon_y}. \tag{12}$$

2.3.2. Flexural overstrength factor for RHS and SHS profiles

A number of predictive equations for evaluating flexural overstrength of steel beams with RHS and SHS profiles are available in the literature

Table 1
Summary of the experimental database for the I–H and RHS–SHS steel beams.

No.	Authors	Test no.	Profile type	Steel grade	Test setup	Loading history
1	Lukey and Adams (1969) [35]	12	I and H hot-rolled	MCS[a]	3PBT[c]	Monotonic
2	Climenhaga (1970) [36]	10	I welded	MCS	3PBT	Monotonic
3	Grubb and Carskaddan (1979,1981) [37,38]	7	I welded	HSS[b]	3PBT	Monotonic
4	Kemp (1985) [39]	14	I and H welded + hot-rolled	MCS	3PBT	Monotonic
5	Schilling (1988,1990) [40,41]	3	I welded	HSS	3PBT	Monotonic
6	Wargsjö (1991) [42]	10	I welded	HSS	3PBT	Monotonic
7	Dahl et al. (1992) [43]	6	I welded	HSS	3PBT	Monotonic
8	Boeraeve and Lognard (1993) [44]	5	I and H hot-rolled	MCS	3PBT	Monotonic
9	Suzuki et al. (1994) [45]	6	I welded	MCS + HSS	3PBT	Monotonic
10	Landolfo et al. (2011) [1,46]	3	I and H hot rolled	MCS	CBT[e]	Monotonic
11	Wilkinson (1999) [29]	44	Cold-formed RHS + SHS	MCS	4PBT[d]	Monotonic
12	Zhou and Young (2005) [47]	15	Cold-formed RHS + SHS	MCS + HSS	4PBT	Monotonic
13	Landolfo et al. (2011) [1,46]	6	Cold-formed RHS + SHS	MCS	CBT	Monotonic

[a] MCS = mild carbon steel.
[b] HSS = high-strength steel.
[c] 3PBT = 3-point bending test.
[d] 4PBT = 4-point bending test.
[e] CBT = cantilever bending test.

Table 2
Input and output database of training and test sets for I–H steel beams.

Ref no.	Data no.	b_f	d	t_f	t_w	L_v	$f_{y,\ flange}$	$f_{y,\ web}$	E/E_h	$\varepsilon_h/\varepsilon_y$	s
[35]	1	203.5	256.7	10.8	7.65	1740	283	308	42.8	11	1.38
	2	176	256.7	10.8	7.65	1473	283	308	42.8	11	1.41
	3	102.6	201.86	5.28	4.45	777	371	395	48.2	9.8	1.11
	4	73.9	201.86	5.28	4.45	518	371	395	48.2	9.8	1.15
	5	86.1	201.86	5.28	4.45	627	371	395	48.2	9.8	1.13
	6	94	201.86	5.28	4.45	698	371	395	48.2	9.8	1.05
	7	96.8	201.82	5.26	4.45	724	371	395	48.2	9.8	1.04
	8	101.9	251.72	5.26	4.6	686	371	350	48.2	9.8	1.11
	9	73.7	251.72	5.26	4.6	480	371	350	48.2	9.8	1.26
	10	85.9	251.72	5.26	4.6	584	371	350	48.2	9.8	1.16
	11	93.5	251.72	5.26	4.6	648	371	350	48.2	9.8	1.12
	12	88.9	251.72	5.26	4.6	640	371	350	48.2	9.8	1.14
[36]	13	135	201	8	5.7	1956	315	344	48.2	9.8	1.09
	14	134	204	9.5	6	1956	293	310	42.8	11	1.22
	15	104	305.8	6.9	6	1956	357	412	48.2	9.8	0.89
	16	128	352	8	6	1956	324	363	48.2	9.8	0.86
	17	141	398.2	7.6	6.2	1956	303	379	42.8	11	0.92
	18	135	201	8	5.7	1346	315	344	48.2	9.8	1.06
	19	134	204	9.5	6	1346	293	310	42.8	11	1.26
	20	104	305.8	6.9	6	1346	357	412	48.2	9.8	0.97
	21	128	352	8	6	1346	324	363	48.2	9.8	0.92
	22	105	308.6	10.3	6.2	1346	319	384	48.2	9.8	0.97
[37,38]	23	156	406.4	9.7	6.7	914	383	345	48.2	9.8	1.04
	24	156	406.4	9.7	6.7	1829	383	345	48.2	9.8	1.00
	25	156	406.4	9.7	6.7	2743	383	345	48.2	9.8	0.96
	26	157	308.4	11.2	8.3	1219	370	337	48.2	9.8	1.31
	27	150	374.4	11.2	8.4	1524	370	337	48.2	9.8	1.15
	28	130	404.4	11.2	8.4	1524	370	337	48.2	9.8	1.10
	29	158	407.4	11.2	8.4	1524	370	337	48.2	9.8	1.08
[39]	30	150	217.8	8.09	6.65	1830	340	358	48.2	9.8	1.12
	31	145	217.4	10.57	6.82	1830	285	329	42.8	11	1.14
	32	106	273.9	7.05	5.85	1830	332	388	48.2	9.8	1.03
	33	149	217.9	8.56	6.78	915	340	358	48.2	9.8	1.27
	34	149	217.1	8.44	6.78	915	294	300	42.8	11	1.22
	35	140	209.5	10.77	6.76	915	288	329	42.8	11	1.27
	36	145	366.3	8.33	5.96	1830	375	403	48.2	9.8	1.01
	37	154	120.3	9.83	7.44	1830	313	300	48.2	9.8	1.22
	38	146	217.9	9.03	6.35	1830	340	358	48.2	9.8	1.09
	39	105	282.2	6.92	5.82	1830	332	388	48.2	9.8	1.00
	40	104	277.5	6.76	5.59	2179	317	351	48.2	9.8	1.05
	41	145.54	402.2	11.11	6.84	1830	285	329	42.8	11	1.11
	42	180	210	8.05	6.11	1830	332	326	48.2	9.8	1.18
	43	180	210	8	6	1816	332	326	48.2	9.8	1.26
[40,41]	44	127	611	7	5.3	1067	410	450	48.2	9.8	0.68
	45	229	622	12.5	5.3	1981	401	450	48.2	9.8	0.81
	46	311	945.4	15.7	5.3	2895.5	342	450	48.2	9.8	0.89
[42]	47	131	500.8	9.9	4	1910	370	335	48.2	9.8	0.91
	48	130	501.8	9.9	4	2860	370	335	48.2	9.8	0.89
	49	131	457	10	4	1760	370	335	48.2	9.8	0.92
	50	131	458.8	9.9	4	2640	370	335	48.2	9.8	0.95
	51	132	414.6	9.8	4	1610	370	335	48.2	9.8	0.94
	52	130	422	10	4	2400	370	335	48.2	9.8	0.92
	53	131	379.8	9.9	4	1460	370	335	48.2	9.8	0.99
	54	131	379.8	9.9	4	2160	370	335	48.2	9.8	0.97
	55	131	336	10	4	1310	370	335	48.2	9.8	1.02
	56	131	339.6	9.8	3.9	1920	370	335	48.2	9.8	0.98
[43]	57	202	200	15	9.5	1500	428	456	48.2	9.8	1.36
	58	202	200	15	9.5	1500	428	456	48.2	9.8	1.30
	59	280	280	18	10	1500	982	984	48.2	9.8	1.09
	60	280	280	18	10	1500	864	813	48.2	9.8	1.06
	61	280	280	18	10	1500	468	536	48.2	9.8	1.06
	62	280	280	18	10	1500	278	323	48.2	9.8	1.24
[44]	63	200.7	183.3	14.1	8.8	1500	303	342	42.8	11	1.14
	64	200.2	183.3	14.7	9.5	1500	375	421	48.2	9.8	1.15
	65	201.5	184.6	15.1	9.5	1500	445	462	48.2	9.8	1.16
	66	200.4	185.8	14.6	9.6	1500	261	291	37.5	12.3	1.13
	67	199.9	189.3	14.9	9.4	1500	409	426	48.2	9.8	1.15
[45]	68	150	132	9	6	600	291	340	42.8	11	1.25
	69	150	132	9	6	900	291	340	42.8	11	1.23
	70	150	132	9	6	600	526	509	48.2	9.8	1.26
	71	150	132	9	6	600	527	340	48.2	9.8	1.20
	72	150	132	9	6	600	291	509	42.8	11	1.15
	73	150	132	9	6	900	291	686	42.8	11	1.14

(continued on next page)

Table 2 (*continued*)

Ref no.	Data no.	b_f	d	t_f	t_w	L_v	$f_{y,\ flange}$	$f_{y,\ web}$	E/E_h	$\varepsilon_h/\varepsilon_y$	s
[1,46]	74	160	152	9	6	1875	275	275	42.8	11	1.30
	75	240	240	17	10	1875	275	275	42.8	11	1.36
	76	150	300	10.7	7.1	1875	275	275	42.8	11	1.22

Table 3
Input and output database of training and test sets for RHS–SHS steel beams.

Ref no.	Data no.	b	d	t	r	L_v	f_y	E/E_h	$\varepsilon_h/\varepsilon_y$	s
[29]	1	50.25	151.04	4.92	9.9	450	441	48.2	9.8	1.23
	2	50.41	150.92	4.9	10.7	450	441	48.2	9.8	1.17
	3	50.27	150.43	3.92	6.8	450	457	48.2	9.8	1.27
	4	50.4	150.44	3.87	7.3	450	457	48.2	9.8	1.19
	5	50.11	150.42	3.89	7.3	450	457	48.2	9.8	1.24
	6	50.16	150.21	3.89	5.4	450	423	48.2	9.8	1.17
	7	50.22	150.47	2.97	5.9	450	444	48.2	9.8	1.15
	8	50.01	150.79	2.95	5.8	450	444	48.2	9.8	1.16
	9	50.34	150.8	2.96	5.7	450	444	48.2	9.8	1.13
	10	50.15	150.43	2.6	4.6	450	446	48.2	9.8	1.02
	11	50.41	150.39	2.57	4.6	450	446	48.2	9.8	1.00
	12	50.23	150.4	2.59	4.8	450	446	48.2	9.8	1.10
	13	50.4	150.31	2.64	5.3	450	440	48.2	9.8	1.11
	14	50.64	150.65	2.25	4.6	450	444	48.2	9.8	0.98
	15	50.57	150.51	2.28	4.2	450	444	48.2	9.8	1.01
	16	50.7	150.37	2.26	4.8	450	444	48.2	9.8	0.98
	17	50.7	100.45	2.06	3.8	450	449	48.2	9.8	1.07
	18	50.55	100.49	2.07	3.9	450	449	48.2	9.8	1.01
	19	50.24	100.46	2.04	4.7	450	449	48.2	9.8	1.07
	20	50.22	100.45	2.04	3.4	450	423	48.2	9.8	1.08
	21	50.1	75.48	1.94	4.4	400	411	48.2	9.8	1.04
	22	50.31	75.63	1.95	4.4	400	411	48.2	9.8	1.02
	23	25.28	75.31	1.98	3.7	400	457	48.2	9.8	1.11
	24	25.23	75.33	1.95	4	400	457	48.2	9.8	1.13
	25	25.12	75.24	1.54	3.1	400	439	48.2	9.8	1.08
	26	25.2	74.9	1.54	3.4	400	439	48.2	9.8	1.13
	27	25.08	74.98	1.56	3.9	400	439	48.2	9.8	1.09
	28	25.12	75.27	1.55	3.4	400	422	48.2	9.8	1.03
	29	25.25	75.19	1.56	3.4	400	422	48.2	9.8	1.00
	30	50.13	150.46	3	6.2	450	370	48.2	9.8	1.21
	31	50.19	150.5	2.96	6.5	450	370	48.2	9.8	1.15
	32	50.51	150.45	3	6.8	450	382	48.2	9.8	1.18
	33	50.51	150.38	3	6.3	450	382	48.2	9.8	1.21
	34	50.43	100.91	2.06	3.6	450	400	48.2	9.8	1.00
	35	50.52	100.83	2.05	3.8	450	400	48.2	9.8	1.00
	36	75.84	125.56	2.92	6.6	450	397	48.2	9.8	1.03
	37	75.74	125.4	2.93	6.9	450	397	48.2	9.8	1.04
	38	75.56	125.4	2.91	7.1	450	397	48.2	9.8	1.03
	39	75.1	125.4	2.53	3.9	450	374	48.2	9.8	1.06
	40	100.27	100.43	2.88	5.2	450	445	48.2	9.8	1.02
	41	100.33	100.53	2.91	5	450	445	48.2	9.8	0.95
	42	100.25	100.53	2.86	5.2	450	445	48.2	9.8	1.03
	43	50.21	150.32	3.9	7.9	450	349	48.2	9.8	1.28
	44	50.57	150.39	3.85	7.5	450	410	48.2	9.8	1.19
[47]	45	40.1	40.1	1.96	2	480.7	447	48.2	9.8	1.29
	46	40	40.1	3.88	4	480.3	565	48.2	9.8	1.31
	47	80.5	80.4	1.91	4	480.7	398	48.2	9.8	0.98
	48	79.9	79.8	4.77	7.5	481	448	48.2	9.8	1.49
	49	49.8	99.9	1.97	2	480	320	48.2	9.8	1.51
	50	49.6	99.7	3.88	4	479.7	378	48.2	9.8	1.71
	51	59.9	120.2	1.84	2.5	480.7	361	48.2	9.8	1.14
	52	59.7	120	3.89	5.5	480.7	392	48.2	9.8	1.80
	53	40.2	40	1.94	2	414.3	707	48.2	9.8	1.21
	54	50.1	50.3	1.54	1.5	414	622	48.2	9.8	1.05
	55	150.6	150.7	2.78	4.8	546.7	448	48.2	9.8	0.78
	56	150.7	150.5	5.87	6	550	497	48.2	9.8	1.23
	57	80.5	140.3	3.09	6.5	480	486	48.2	9.8	1.19
	58	80.9	160.6	2.9	6	480	536	48.2	9.8	1.07
	59	109.1	197.7	4	8.5	548	503	48.2	9.8	1.07
[1,46]	60	100	150	5	10	1875	275	42.6	11	1.29
	61	80	160	4	8	1875	275	42.6	11	1.25
	62	100	250	10	20	1875	275	42.6	11	1.44
	63	160	160	6.3	12.6	1875	355	48.2	9.8	1.05
	64	200	200	10	20	1875	355	48.2	9.8	1.28
	65	250	250	8	16	1875	355	48.2	9.8	1.14

[1,2,25,26]. For example, Kato [25,26] proposed a relationship generalised for cold-formed SHS, given by the following:

$$\frac{1}{s} = 0.778 + \frac{0.13}{\alpha} \tag{13}$$

where

$$\alpha = \frac{E}{f_y}\left(\frac{t}{b}\right)^2 \tag{14}$$

is the slenderness parameter for the SHS section, with b being the width of the edge in compression and t being the corresponding thickness.

Brescia [2] proposed a formulation for s obtained by multi-linear regression analysis of the experimental data obtained from tests carried out by Wilkinson [29] on cold-formed profiles. Thus, the following expressions were provided:

$$\frac{1}{s} = 0.711 + 0.09\lambda_f^2 + 0.318\lambda_w^2 - 0.189\frac{b_f}{L_v} \quad \text{for SHS beams} \tag{15}$$

$$\frac{1}{s} = 2.7 + 0.62\lambda_f^2 + 0.0206\lambda_w^2 - 2.11\frac{b_f}{L_v} \quad \text{for RHS beams.} \tag{16}$$

More recently, based on a wider experimental database, D'Aniello et al. [1] proposed a unique equation to estimate the flexural overstrength factor for RHS and SHS steel beams, given as follows:

$$\frac{1}{s} = 0.014 + 0.294\lambda_f^2 + 0.094\lambda_w^2 - 0.713\frac{b_f}{L_v} + 0.017\frac{E}{E_h}. \tag{17}$$

3. Overview of genetic programming

A genetic algorithm (GA) is a search technique used in computing to find precise or approximate solutions to optimisation or search problems. GAs are a particular class of evolutionary computation and can be categorised as global search heuristics. The techniques used by GA are inspired by evolutionary biology, including inheritance, mutation, selection, and crossover (recombination).

Genetic programming (GP) is essentially the application of genetic algorithms to computer programmes [30]. GP has been applied successfully to solve discrete, non-differentiable, combinatory, and general nonlinear engineering optimisation problems [31]. It is an evolutionary algorithm-based methodology inspired by biological evolution used to develop a computer programme that performs a user-defined task. Therefore, it is a machine-learning technique used to create a population of computer programmes according to a fitness landscape determined by a programme's ability to perform a given computational task. Similar to GA, the GP only needs the problem to be defined as input. Next, the programme searches for a solution in a problem-independent manner [30,32].

Gene expression programming (GEP), introduced by Ferreira [33], can be considered a natural development of genetic algorithms and genetic programming. In detail, GEP evolves computer programmes of different sizes and shapes encoded in fixed-length linear chromosomes. A GEP algorithm begins with a random generation of the fixed-length chromosomes of each individual in the initial population. Next, the

Table 4
Statistics for the experimental data for I–H steel beams.

	b_f	d	t_f	t_w	L_v	$f_{y,\ flange}$	$f_{y,\ web}$	E/E_h	$\varepsilon_h/\varepsilon_y$	s
a) Training data										
No. of data	57	57	57	57	57	57	57	57	57	57
Mean	145.89	286.65	9.84	6.39	2905.65	374.28	380.16	46.97	10.08	1.09
Standard deviation	44.34	111.85	3.22	1.85	1098.23	118.88	112.16	2.50	0.56	0.14
COV	0.30	0.39	0.33	0.29	0.38	0.32	0.30	0.05	0.06	0.13
Min. value	73.70	120.30	5.26	3.90	960	261	275	37.50	9.80	0.68
Max. value	280.00	622.00	18.00	10.00	5486.00	982.00	984.00	48.20	12.30	1.36
b) Test data										
No. of data	19	19	19	19	19	19	19	19	19	19
Mean	169.64	301.45	10.11	6.32	3166.26	337.47	383.05	46.49	10.18	1.12
Standard deviation	62.24	189.84	3.82	1.81	1318.66	50.25	99.43	2.58	0.57	0.15
COV	0.37	0.63	0.38	0.29	0.42	0.15	0.26	0.06	0.06	0.13
Min. value	88.9	132.0	5.3	4.0	1200.0	275.0	275.0	42.8	9.8	0.9
Max. value	311	945	18	10	5791	468	686	48	11	1

Table 5
Statistics for the experimental data for RHS–SHS steel beams.

	b_f	d	t	r	L_v	f_y	E/E_h	$\varepsilon_h/\varepsilon_y$	s
a) Training data									
No. of data	49	49	49	49	49	49	49	49	49
Mean	63.43	123.94	2.96	5.68	532.39	420.82	48.09	9.82	1.13
Standard deviation	41.64	37.08	1.58	3.18	347.26	39.73	0.80	0.17	0.17
COV	0.66	0.30	0.53	0.56	0.65	0.09	0.02	0.02	0.15
Min. value	25.08	74.90	1.54	2.00	400.00	320.00	42.60	9.80	0.95
Max. value	250.00	250.00	10.00	20.00	1875.00	536.00	48.20	11.00	1.80
b) Test data									
No. of data	16	16	16	16	16	16	16	16	16
Mean	74.57	128.89	3.96	6.94	736.85	445.38	47.15	10.03	1.19
Standard deviation	37.61	61.26	2.03	4.47	566.25	121.14	2.26	0.48	0.16
COV	0.50	0.48	0.51	0.64	0.77	0.27	0.05	0.05	0.13
Min. value	40	40	1.54	1.50	414	275	42.60	9.80	0.78
Max. value	150.70	250	10	20	1875	707	48.20	11.00	1.44

chromosomes are expressed, and the fitness of each individual is evaluated based on the quality of the solution it represents [34]. Based on GEP, novel formulations for the flexural overstrength of steel beams are proposed hereinafter.

4. Proposed GEP formulation

New formulations of the flexural overstrength factor (s) for I–H and RHS–SHS steel beams were derived using a set of experimental data available in the technical literature [1,35–47]. The examined test configurations, accounting for different load patterns (namely, bending moment distribution) are depicted in Figs. 2 and 3. The data sources presented in Table 1 contain precisely selected data samples to ensure a wide range of cross-section typologies under monotonic loading with different local slenderness ratios. The experimental data are reported in Tables 2 and 3 for I–H and RHS–SHS beams, respectively. All of the data samples were ordered to create a consistent sequence of the inputs to be used for the derivation of the models. The input nodes include the geometric properties of the section, the mechanical properties of the material, and the shear length of the steel beams. Thus, nine and eight input parameters were utilised for the development of GEP models for the I–H and RHS–SHS profiles, respectively.

The model generated for I–H sections consists of the following parameters: b_f (width of flange), d (depth of section), t_f (thickness of flange), t_w (thickness of web), L_v (shear length), $f_{y,\ flange}$ (yield stress of flange), $f_{y,\ web}$ (yield stress of web), E/E_h (ratio of the modulus of elasticity of steel to the hardening modulus), and $\varepsilon_h/\varepsilon_y$ (ratio of the strain corresponding to the beginning of hardening to the yield strain) (Table 2).

The GEP model for the RHS–SHS profiles included the following input parameters: b (width of section), d (depth of section), t (wall thickness of section), r (inside corner radius), L_v (shear length), f_y (yield stress), E/E_h, and $\varepsilon_h/\varepsilon_y$ (Table 3).

The development of a genetic-programming-based mathematical formulation is achieved using the training data containing input and output variables. Moreover, to examine and test the performance of the generated model, an optional data set containing the same number and sequence of input and output variables is used. Therefore, in the current study, two ensembles of available experimental data (one for I–H and one for RHS–SHS beams) were arbitrarily divided into two parts to obtain the training and testing databases. Approximately 1/4

Table 6
GEP parameters used for the proposed models.

Parameter		s for I–H profiles	s' for RHS–SHS profiles
P1	Function set	+, −, *, /, √, ^, ln, exp, sin, cos, tan, arctan	+, −, *, /, √, ^, ln, exp, sin, cos, tan, arctan
P2	Number of generation	492,531	478,574
P3	Chromosomes	30	30
P4	Head size	10	10
P5	Linking function	Addition	Addition
P6	Number of genes	8	8
P7	Mutation rate	0.044	0.044
P8	Inversion rate	0.1	0.1
P9	One-point recombination rate	0.3	0.3
P10	Two-point recombination rate	0.3	0.3
P11	Gene recombination rate	0.1	0.1
P12	Gene transposition rate	0.1	0.1

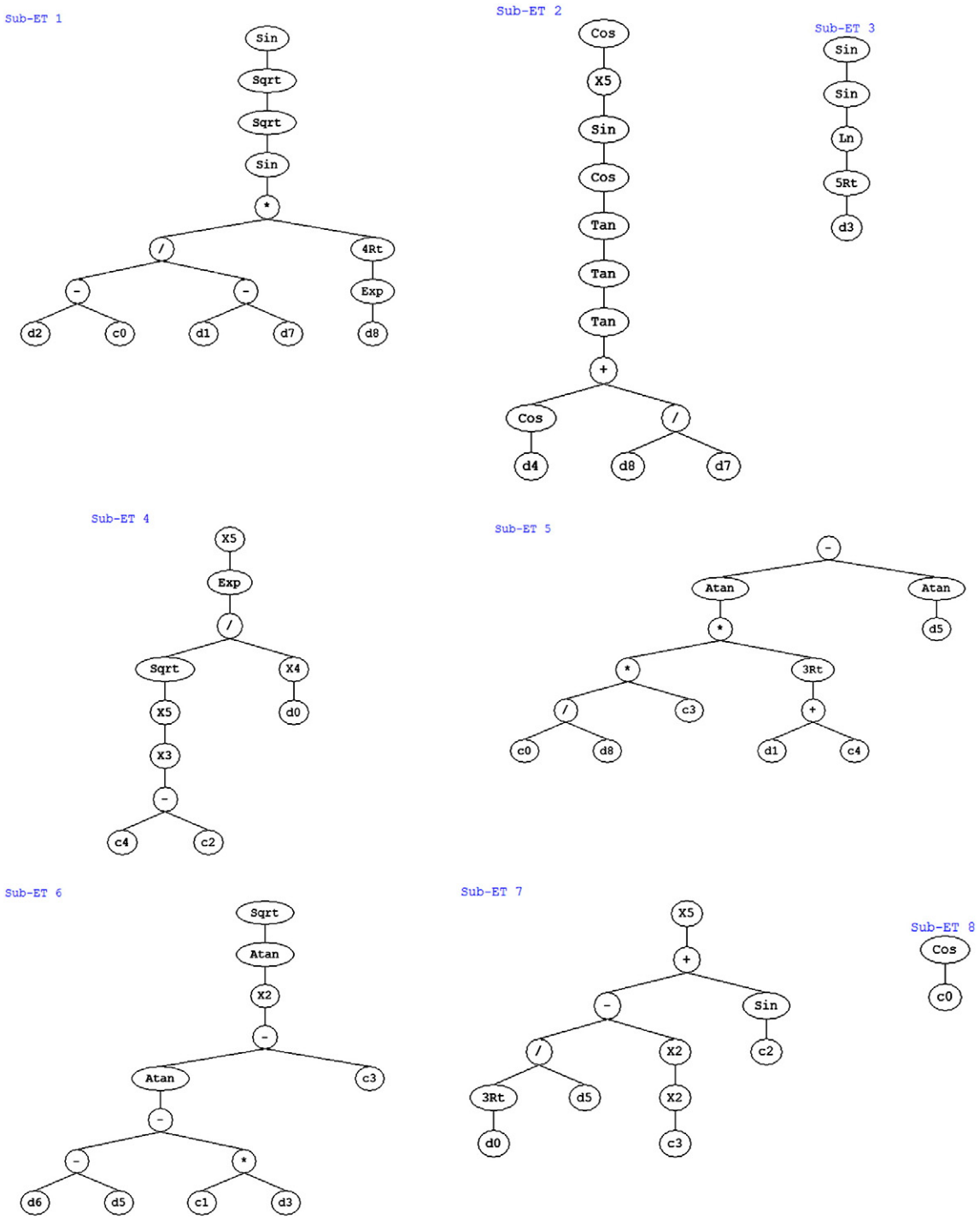

Fig. 4. GEP model expression tree for I–H steel beams.

of the total data samples were used as the test database, while the rest were used as the training database, as shown in Tables 2 and 3. Thus, 57 and 49 data samples were used as the training data for I–H and RHS–SHS profiles, respectively, and the testing database contained 19 data samples for the former and 16 for the latter. The statistical analyses of the data presented in Tables 2 and 3 are summarised in Tables 4 and 5, respectively. As can be observed in Tables 4 and 5, the statistics for both the training and testing sets are in good agreement, meaning that both of them represent almost identical populations.

GeneXproTools 4.0 software was utilised for the derivation of the mathematical model. The GEP parameters used for the derivation of the mathematical models are given in Table 6. As seen from Table 6, to provide an accurate model, various mathematical operations were used. Several modifications of the GEP parameters have been made to obtain an optimum model with the best fitness. However, trigonometric operations in combination with exponential functions were predominantly included in the GEP models presented in this study.

The correlation coefficient (R) (Eq. (18)) describes the fit of the GEP's output variable approximation curve to the actual test data output

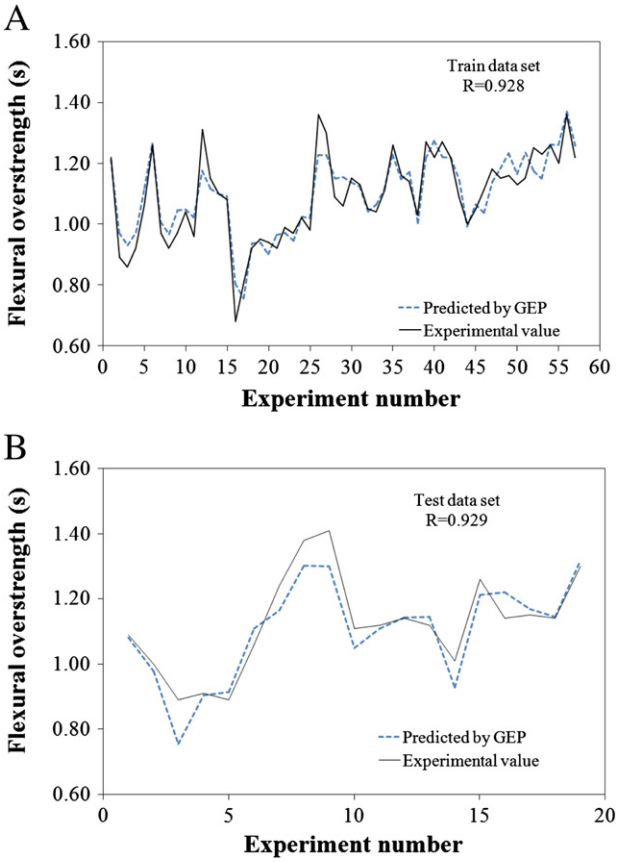

Fig. 5. Evaluation of the experimental and predicted flexural overstrength factors for I–H steel beams: A) training set and B) test set.

variable curve. Higher R coefficients indicate a model with better output approximation capability.

$$R = \frac{\sum (m_i - m')(p_i - p')}{\sqrt{\sum (m_i - m')^2 \sum (p_i - p')^2}} \tag{18}$$

where m' and p' are the means of the measured (m_i) and predicted (p_i) values, respectively.

4.1. GEP formulation for I and H beams

The prediction model for I–H sections derived from GEP is presented in Eq. (19). The models developed by the software in its native language can be automatically parsed into visually appealing expression trees, permitting a quicker and more complete comprehension of their mathematical/logical intricacies. Fig. 4 demonstrates the expression tree for the terms used in the formulation of the GEP model. In the expression tree given in Fig. 4, each of the first seven sub-parts of the tree contains various input variables. However, Sub-ET 8 has no independent variable and is instead the cosine of a real number. Therefore, S_8 in the mathematical model was taken as a constant input, −0.51304.

The performance of the proposed GEP prediction model in Eq. (19) was graphically depicted in Fig. 5 for both the training and testing data sets. The variations of the predicted and experimental data are strongly correlated, with correlation coefficients of 0.928 and 0.929 for the training and testing databases, respectively. Moreover, the closeness of the values of the correlation coefficients may also be considered as evidence for the consistency and good fitness of the proposed model.

$$s = s_1 + s_2 + s_3 + s_4 + s_5 + s_6 + s_7 + s_8 \tag{19}$$

$$s_1 = \sin\left[\sqrt[4]{\sin\left(\left(\frac{d_2 + 5.179657}{d_1 - d_7}\right) \times \sqrt[4]{e^{d_8}}\right)}\right] \tag{19a}$$

$$s_2 = \cos\left[\left(\sin\left(\cos\left(\tan\left(\tan\left(\tan\left(\cos d_4 + d_8/d_7\right)\right)\right)\right)\right)\right)^5\right] \tag{19b}$$

$$s_3 = \sin\left(\sin\left(\ln\left(\sqrt[5]{d_3}\right)\right)\right) \tag{19c}$$

$$s_4 = \left[e^{\frac{898348.077}{d_0^4}}\right]^5 \tag{19d}$$

$$s_5 = \arctan\left(-\left(\frac{0.159546}{d_8}\right) \times 4.477539 \times \sqrt[3]{d_1 - 9.755524}\right) - \arctan(d_5) \tag{19e}$$

$$s_6 = \sqrt{\arctan\left(\left(\arctan(d_6 - d_5 - 4.202667 \times d_3) - 3.717102\right)^2\right)} \tag{19f}$$

$$s_7 = \left(\frac{\sqrt[3]{d_0}}{d_5} - 0.9484470303\right)^5 \tag{19g}$$

$$s_8 = -0.51304 \tag{19h}$$

where $d_0 = b_f$ (the flange width, expressed in mm); $d_1 = d$ (the section depth, expressed in mm); $d_2 = t_f$ (the flange thickness, expressed in mm); $d_3 = t_w$ (the web thickness, expressed in mm); $d_4 = L_v$ (the shear length, equal to $L/2$ for the 3-point bending test (3PBT) and L for the cantilever beam test (CBT), with L, the beam length, expressed in mm); $d_5 = f_{y,\ flange}$ (the flange yield stress, expressed in MPa); $d_6 = f_{y,\ web}$ (the web yield stress, expressed in MPa); $d_7 = E/E_h$ (the ratio of the modulus of elasticity of steel to the hardening modulus); and $d_8 = \varepsilon_h/\varepsilon_y$ (the ratio of the strain corresponding to the beginning of hardening to the yield strain).

4.2. GEP formulation for RHS and SHS beams

The mathematical formulation of the s value for the RHS–SHS profiles is given in Eq. (20). The expression tree for the model is depicted in Fig. 6, while the prediction performance of the model is shown in Fig. 7. The calculated correlation coefficients (R) are equal to 0.922 and 0.909 for the training and testing datasets, respectively. Although the R values for this model are slightly lower than those obtained from the previous model, the proposed model appeared to be sufficient for predicting the s value for the RHS–SHS sections.

$$s' = s'_1 + s'_2 + s'_3 + s'_4 + s'_5 + s'_6 + s'_7 + s'_8 \tag{20}$$

$$s'_1 = \left(\frac{\sin(d_1 - d_4 \times d_6 + 4.326019 + d_2)}{1.495056}\right)^4 \tag{20a}$$

$$s'_2 = \frac{d_2}{\left[2.046875 - \frac{\tan\left(\sqrt[3]{d_4}\right)}{d_5/d_3}\right] \times d_3} \tag{20b}$$

$$s'_3 = \left(\frac{d_6}{d_5}\right)^3 \times \cos d_1 \times \sqrt[5]{d_4^2} - 4.395874 \tag{20c}$$

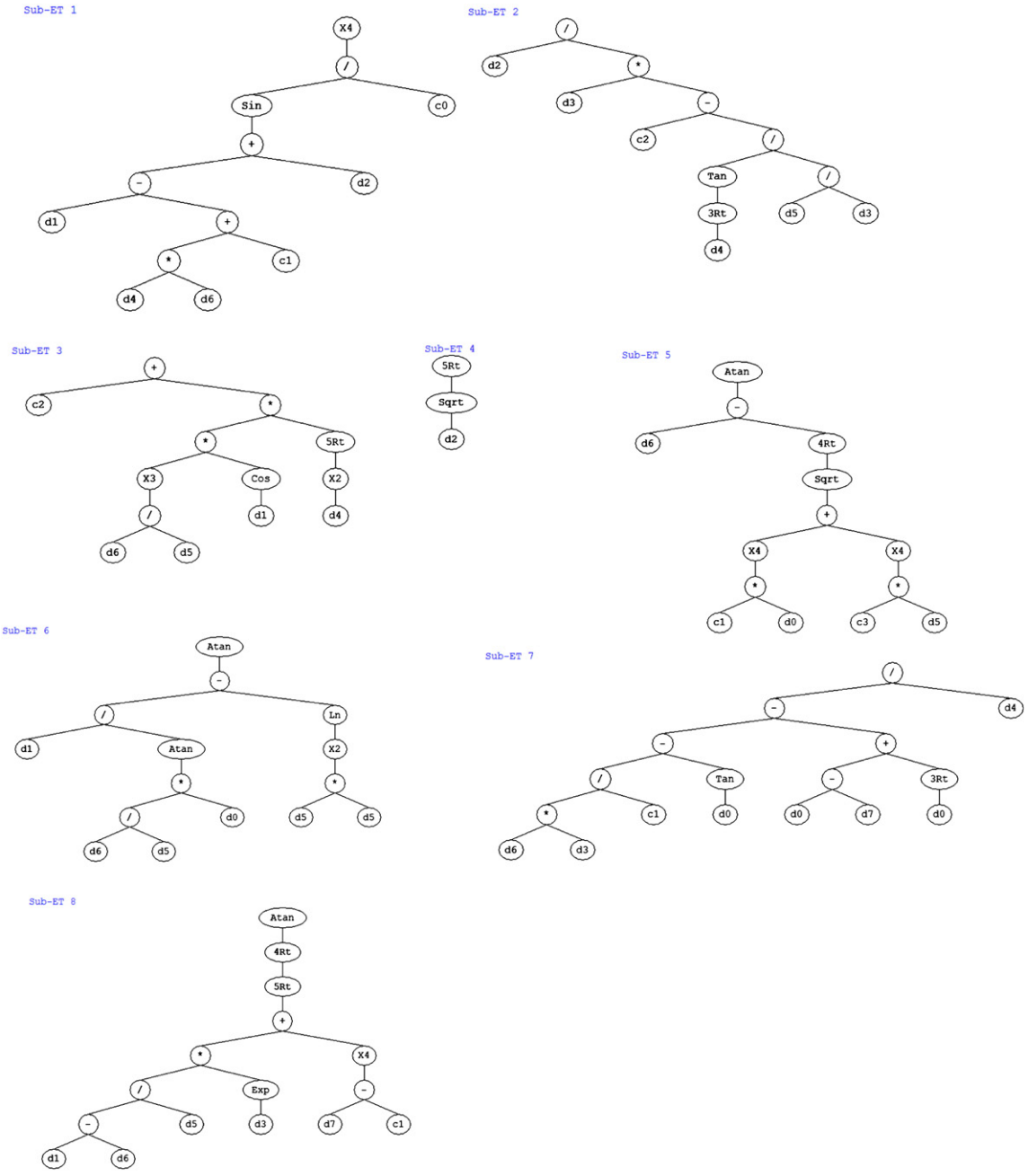

Fig. 6. GEP model expression tree for RHS–SHS steel beams.

$$s'_4 = \sqrt[10]{d_2} \tag{20d}$$

$$s'_5 = \arctan\left[d_6 - \sqrt[8]{(7.417725 \times d_0)^4 + (2.573029 \times d_5)^4}\right] \tag{20e}$$

$$s'_6 = \arctan\left[\frac{d_1}{\arctan\left(\frac{d_6 \times d_0}{d_5}\right)} - 4\ln(d_5)\right] \tag{20f}$$

$$s'_7 = \frac{\frac{d_6 \times d_3}{7.647492} - \tan d_0 - d_0 + d_7 - \sqrt[3]{d_0}}{d_4} \tag{20g}$$

$$s'_8 = \arctan\left[\sqrt[20]{\frac{(d_1 - d_6)}{d_5} \times e^{d_3} + (d_7 + 9.994324)^4}\right] \tag{20h}$$

where $d_0 = b$ (the section width, expressed in mm); $d_1 = d$ (the section depth, expressed in mm); $d_2 = t$ (the section wall thickness, expressed in mm); $d_3 = r$ (the inside corner radius, expressed in mm); $d_4 = L_v$ (the shear length, equal to $(L_1 - L_2)/2$ for the 4-point bending test (4PBT) and L for the CBT test, where L_1 and L_2 are described in Fig. 3 and expressed in mm); $d_5 = f_y$ (the yield stress, expressed in MPa); $d_6 = E/E_h$ (the ratio of the modulus of elasticity of steel to the hardening modulus); and $d_7 = \varepsilon_h/\varepsilon_y$ (the ratio of the strain corresponding to the beginning of hardening to the yield strain).

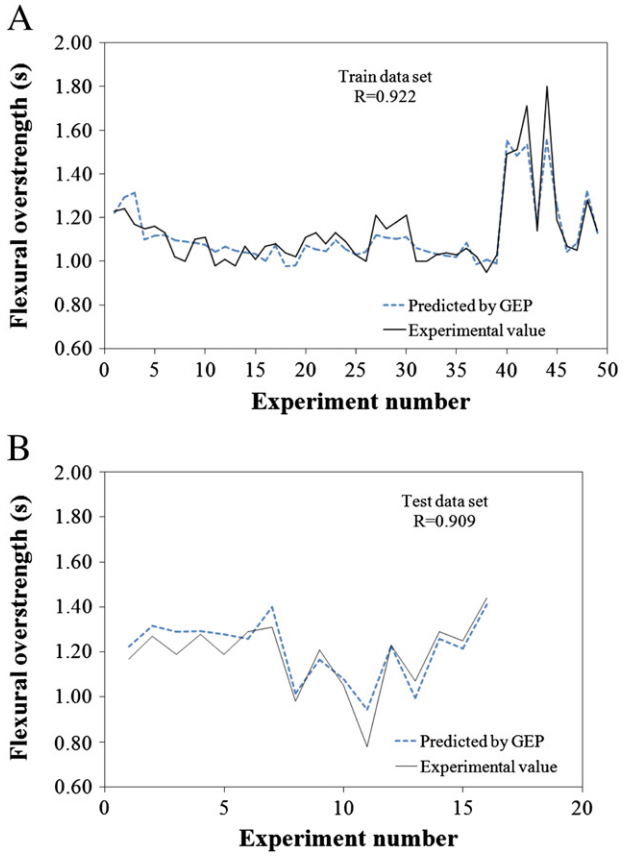

Fig. 7. Evaluation of the experimental and predicted flexural overstrength factors for RHS–SHS steel beams: A) training set and B) test set.

5. Discussion of results

To evaluate the efficiency and accuracy of the proposed formulations, the prediction performances of the GEP models and that from existing analytical formulations (described in Section 2.3) are compared to the experimental data for I–H and RHS–SHS steel beams. Figs. 8 and 9 indicate the fluctuations of normalised overstrength factors versus experimental values for I–H and RHS–SHS steel beams, respectively. Hereinafter, the unique characteristics of each case are described and discussed.

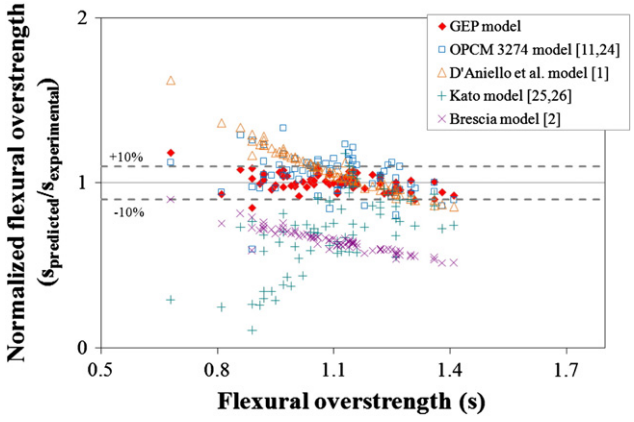

Fig. 8. Prediction performance of the GEP model and existing models for I–H steel beams.

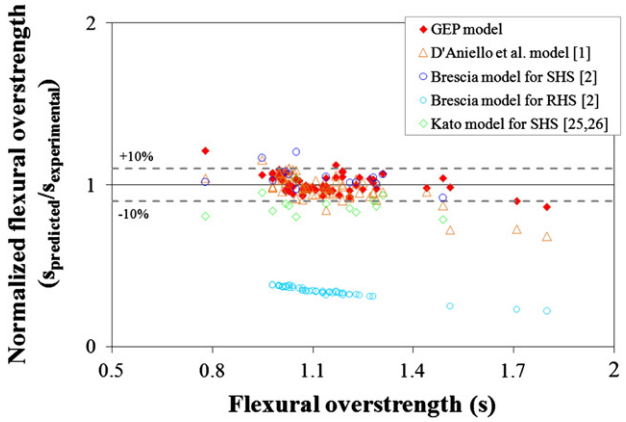

Fig. 9. Prediction performance of the GEP model and existing models for RHS–SHS steel beams.

5.1. GEP model vs. existing analytical formulations for I–H sections

As it can be observed in Fig. 8, the predicted values of *s* for the GEP model ranged from 0.85 to 1.18. However, the ranges of variation for the other models were as follows: 0.59–1.33 for OPCM 3274 [11,24], 0.85–1.62 for the D'Aniello et al. model [1], 0.11–1.17 for the Kato model [25,26], and 0.51–0.90 for the Brescia model [2]. Among the prediction formulations, the proposed GEP model has a correlation coefficient closest to 1.0. Moreover, Fig. 8 shows that, except the most extreme upper and lower values, all of the normalised overstrength factors obtained from the GEP model fall within ± 10%. Although the OPCM 3274 [11,24] model yielded fluctuating values that are not far from the ±10% limit, its prediction was worse than that of the GEP model. The results obtained from the D'Aniello et al. model [1] tended to decrease as the actual *s* values increased. However, for *s* values of approximately 1.1, the predicted values are almost identical to the exact values. However, for actual values greater than 1.1, the model tends to underestimate the strength factors, while for actual values less than 1.1, this model overestimates these values. A non-uniform underestimated scatter of the normalised values are observed in the Kato model [25,26]. Moreover, the obtained results are strongly divergent from the actual values. Despite having a regular tendency, the normalised values obtained from the Brescia model [2] are lower than the actual values.

5.2. GEP model vs. existing analytical formulations for RHS–SHS profiles

Based on a critical observation of Fig. 9, it can be inferred that the prediction models provide reasonable estimation performance, except for the Brescia model for RHS [2]. For experimental values of *s* ranging from 0.95 to 1.31, the GEP model and the model by D'Aniello et al. [1] give similar values, which are very close to the actual ones. However,

Table 7
Statistical parameters of the proposed and existing analytical models for I–H steel beams.

Parameters	GEP model		OPCM model	Kato model	Brescia model	D'Aniello et al. model
	Training data set	Testing data set				
Mean square error (MSE)	0.003	0.003	0.016	0.135	0.233	0.019
Mean absolute percent error (MAPE)	4.08	4.04	9.68	30.31	39.71	11.31
Root mean square error (RMSE)	0.054	0.058	0.129	0.367	0.482	0.140

for greater values, the model by D'Aniello et al. [1] tends to underestimate these values. In contrast, the values obtained from the GEP model are still within the −10% limit. The results from the Kato model [25,26] are consistent with the variation of the actual values. Nonetheless, they are generally lower than the actual values. Given that the normalised values obtained from the Brescia model [2] for SHS and RHS are within the ranges of 0.91–1.21 and 0.22–0.38, respectively, it can be concluded that the performance of this model for SHS is much better than that for RHS.

5.3. Statistical analysis of the results

The accuracy of the prediction performance provided by all models was evaluated using statistical analysis. Indeed, the quality of the prediction can usually be characterised by the mean square error (MSE) of the predicted values from the real measured data. The smaller the MSE of both data sets (training and test), the higher the predictive quality. The mean square error (MSE), mean absolute percentage error (MAPE), and root mean square error (RMSE) have been introduced to examine the performance of the models. The statistical formulations of these parameters are given in Eqs. (21) through (23). Lower MAE and MAPE values also show the robustness of the proposed models.

$$MSE = \frac{\sum_{i=1}^{n} (m_i - p_i)^2}{n} \tag{21}$$

$$MAPE = \frac{1}{n}\sum_{i=1}^{n}\left|\frac{m_i - p_i}{m_i}\right| \times 100 \tag{22}$$

$$RMSE = \sqrt{\frac{\sum_{i=1}^{n} (m_i - p_i)^2}{n}} \tag{23}$$

where m' and p' are the mean values of the measured (m_i) and predicted (p_i) values, respectively.

The aforementioned statistical parameters are summarised in Tables 7 and 8 for the prediction models for the I–H and RHS–SHS steel beams, respectively. As can be recognised from the tables, the lowest errors were observed for the proposed GEP models independently of the type of cross section. Table 7 shows that the MAPE of the existing models ranged between 9.68% and 39.71%, while the MAPE of the developed GEP model was approximately 4% for I–H sections. Based on the analysis of the statistical errors, the OPCM model [11,24] seems to be the best of the existing models. However, the errors for the D'Aniello et al. model [1] were very close to the OPCM model [11,24].

Table 8 indicates that although there are minor increases, the lowest errors are still observed for GEP model. Moreover, the errors calculated for the D'Aniello et al. [1] model are very close to those of the GEP model, while there is a sharp increase in the errors for the Brescia [2] model for RHS. Significant reductions for SHS can be observed in the models of Kato [25,26] and Brescia [2]. Again, the lowest error values in the GEP models confirm that the proposed model is more reliable and accurate than the existing formulations.

6. Practical application of the flexural overstrength factor

The proposed GEP models are derived on the basis of monotonic tests of steel beams under different arrangements and bending moment distributions. Although the experimental database is limited to monotonic tests, it can be assumed that the obtained formulations are also suitable under cyclic conditions. Indeed, as examined by [1], the flexural overstrength under cyclic conditions is almost the same for sections classified as class 1 according to Eurocode 3 [48], while it is slightly less than the monotonic for class 2 sections, owing to the occurrence of some degradation phenomena. This aspect implies that the monotonic flexural overstrength factor can be reasonably utilised for seismic capacity design under dissipative structural behaviour concept, where only sections of classes 1 and 2 can be adopted according to Eurocode 8. In all other cases, the monotonic overstrength should be considered as an upper bound.

Hence, both Eqs. (19) and (20) allows the flexural overstrength s to be calculated with adequate accuracy under both monotonic and cyclic loading conditions. These equations can be considered as useful design aids for all cases in which it is necessary to account for strain-hardening effects in failure mode control. In particular, in seismic design, the correct determination of s is fundamental for the application of hierarchy criteria. The field of application of Eqs. (19) and (20) also includes the case of monotonic plastic design, such as the design for robustness, where design rules similar to the hierarchy criteria adopted in seismic design are also needed to ensure the adequate capacity of structural elements under abnormal loading conditions. Hence, to ensure the flexural failure mode of a steel beam, the surrounding members should be designed to resist the maximum bending moment, given by sM_p, which the beam is capable of transferring.

Finally, although the formulations proposed by other researchers are less accurate than those proposed in this paper, it should be noted that such formulations are directly based on non-dimensional parameters having clear physical meaning (flange slenderness, web slenderness, longitudinal stress gradient, etc.). The same parameters have been used for the derivation of the proposed formulations, but the final equations do not clearly show this aspect. In addition, it can be easily recognised that the existing formulations have the advantage of being easily implemented for manual calculations. In contrast, the use of the proposed formulations is less practical due to their complexity and inclusion of several mathematical operations. These considerations suggest that the existing empirical formulations, such as those reported in [1], are more appropriate for code classification purposes. However, thanks to their greater accuracy, the novel proposed models may find effective use as design aids to be implemented through computerisation by users. In such a way, the minor disadvantages due to their high complexity may be easily overcome.

Table 8
Statistical parameters of the proposed and existing analytical models for RHS–SHS steel beams.

Parameters	GEP model		Kato model for SHS	Brescia model		D'Aniello et al. model for RHS + SHS
	Training data set	Testing data set		for SHS	for RHS	
Mean square error (MSE)	0.004	0.004	0.050	0.029	0.577	0.016
Mean absolute percent error (MAPE)	4.39	4.76	14.42	14.53	65.65	6.25
Root mean square error (RMSE)	0.067	0.065	0.223	0.172	0.759	0.125

7. Conclusion

In this paper, a novel and efficient approach for the formulation of the flexural overstrength factor for steel beams made of I–H and hollow profiles is presented. The proposed formulation is based on gene expression programming (GEP) using a wide range of experimental data. Based on the analysis of the prediction performance of the proposed and existing models, the following conclusions can be drawn:

- GEP is a viable method for obtaining a comprehensive mathematical formulation of the flexural overstrength factor for steel beams having different cross-sectional properties.
- The correlation and accuracy of the proposed GEP models for I–H and RHS–SHS profiles are very good. In particular, the correlation coefficients for the training databases are 0.928 and 0.922 for I–H and RHS–SHS profiles, respectively. Moreover, for the testing databases, correlation coefficients of 0.929 for the former and 0.909 for the latter were obtained. Although the database for the testing data set was not used for training, a high level of prediction was obtained for both the training and testing data sets, associated with a low mean absolute percentage of error and high coefficients of correlation. This finding indicates the generalisation capability of the developed model.
- A comparison with the existing analytical formulation for the flexural overstrength highlighted that the GEP models provide the best prediction of the experimental data. Specifically, the Kato [25,26] and Brescia [2] models underestimated the flexural overstrength factor of the I–H sections, while the D'Aniello et al. [1] and OPCM [11,24] formulations demonstrated better accuracy for these sections. For the RHS–SHS sections, all existing models depicted a closer trend if compared to the prediction performances for I–H sections, with the exception of the Brescia model [2] for RHS, which shows a considerable underestimation of the experimental overstrength data.
- Statistical analysis revealed that the proposed GEP formulations have far lower errors than the existing models. In particular, the highest errors are obtained by the Brescia model [2] for both I–H and RHS–SHS profiles.

References

[1] D'Aniello M, Landolfo R, Piluso V, Rizzano G. Ultimate behavior of steel beams under non-uniform bending. J Constr Steel Res 2012;78:144–58.
[2] Brescia M. Rotation capacity and overstrength of steel members for seismic design. University of Naples Federico II; 2008 (PhD Thesis).
[3] Mazzolani FM, Piluso V. Theory and design of seismic resistant steel frames. London: E & FN Spon an imprint of Chapman & Hall; 1996 .
[4] Gioncu V, Mazzolani FM. Ductility of seismic resistant steel structures. London: Spon Press; 2002.
[5] Tortorelli S, D'Aniello M, Landolfo R. Lateral capacity of steel structures designed according to EC8 under catastrophic seismic events. Proceedings of the Final Conference COST ACTION C26: Urban Habitat Constructions under Catastrophic Events, Naples 16–18 2010; 2010.
[6] Della Corte G, D'Aniello M, Landolfo R. Analytical and numerical study of plastic overstrength of shear links. J Constr Steel Res 2013;82:19–32.
[7] Gioncu V, Petcu D. Available rotation capacity of wide-flange beams and beam-columns part 1. Theoretical approaches. J Constr Steel Res 1997;43(1–3):161–217.
[8] Gioncu V, Petcu D. Available rotation capacity of wide-flange beams and beam-columns part 2. Experimental and numerical tests. J Constr Steel Res 1997;43(1–3):219–44.
[9] Gioncu V, Mosoarca M, Anastasiadis A. Prediction of available rotation capacity and ductility of wide-flange beams: part 1: DUCTROT-M computer program. J Constr Steel Res 2012;69:8–19.
[10] Anastasiadis A, Mosoarca M, Gioncu V. Prediction of available rotation capacity and ductility of wide-flange beams: part 2: applications. J Constr Steel Res 2012;68:176–91.
[11] OPCM 3274. First elements in the matter of general criteria for seismic classification of the national territory and of technical codes for structures in seismic zones, Official Gazette of the Italian Republic, Rome, and further modifications; 2003.
[12] Lopes SM, do Carmo RNF. Deformable strut and tie model for the calculation of the plastic rotation capacity. Comput Struct 2006;84:2174–83.
[13] Beg D, Zupancic E, Vayas I. On the rotation capacity of moment connections. J Constr Steel Res 2004;60:601–20.
[14] Mazzolani FM, Piluso V. Prediction of the rotation capacity of aluminium alloy beams. Thin-Walled Struct 1997;27:103–16.
[15] Wilkinson T, Hancock G. Predicting the rotation capacity of cold-formed RHS beams using finite element analysis. J Constr Steel Res 2002;58:1455–71.
[16] Saka MP. Optimum design of pitched roof steel frames with haunched rafters by genetic algorithm. Comput Struct 2003;81:1967–78.
[17] Gholizadeh S, Pirmoz A, Attarnejad R. Assessment of load carrying capacity of castellated steel beams by neural networks. J Constr Steel Res 2011;67:770–9.
[18] Fonseca ET, Vellasco PCGS, de Andrade SAL, Vellasco MMBR. Neural network evaluation of steel beam patch load capacity. Adv Eng Softw 2003;34:763–72.
[19] Gandomi AH, Alavi AH, Kazemi SS, Alinia MM. Behavior appraisal of steel semi-rigid joints using linear genetic programming. J Constr Steel Res 2009;65:1738–50.
[20] Cevik A. Genetic programming based formulation of rotation capacity of wide flange beams. J Constr Steel Res 2007;63:884–93.
[21] AISC 341-10. Seismic provisions for structural steel buildings. American Institute of Steel Construction; 2010.
[22] DM. Nuove Norme Tecniche per le Costruzioni; 2008 (in Italian).
[23] CEN (European Communities for Standardization). EN 1998-1Eurocode 8: design of structures for earthquake resistance—part 1: general rules, seismic actions and rules for buildings; 2005.
[24] Mazzolani FM, Piluso V. Member behavioral classes of steel beams and beam columns. Proc. of First State of the Art Workshop, COST I, Strasbourg; 1992 517–29.
[25] Kato B. Rotation capacity of H-section members as determined by local buckling. J Constr Steel Res 1989;13:95–109.
[26] Kato B. Rotation capacity of steel members subject to local buckling. Proc. of 9th World Conference on Earthquake Engineering, paper 6-2-3, Tokyo-Kyoto; 1988.
[27] Kato B. Deformation capacity of steel structures. J Constr Steel Res 1990;17:33–94.
[28] ASCE. Plastic design in steel: a guide and commentary. Manual and report on engineering practice, no. 41. Welding Research Council and ASCE; 1971 .
[29] Wilkinson T. The plastic behaviour of cold formed rectangular hollow sections. Australia: Department of Civil Engineering, University of Sydney; 1999 (PhD Thesis).
[30] Koza JR. Genetic programming: on the programming of computers by means of natural selection. MIT Press; 1992.
[31] Goldberg D. Genetic algorithms in search, optimization and machine learning. MA: Addison-Wesley; 1989.
[32] Zadeh LA. Soft computing and fuzzy logic. IEEE Softw 1994;11(6):48–56.
[33] Ferreira C. Gene expression programming: a new adaptive algorithm for solving problems. Complex Syst 2001;13(2):87–129.
[34] Özbay E, Gesoğlu M, Güneyisi E. Empirical modeling of fresh and hardened properties of self-compacting concretes by genetic programming. Construct Build Mater 2008;22:1831–40.
[35] Lukey AF, Adams PF. Rotation capacity of beams under moment gradient. J Struct Div 1969;95:1173–88.
[36] Climenhaga JJ. Local buckling in composite beams. Dissertation submitted to the University of Cambridge for the degree of Doctor of Philosophy, Cambridge; 1970.
[37] Grubb MA, Carskaddan PS. Autostress design of highway bridges phase 3: initial moment–rotation tests. AISI project 188, 97-H-045(019-4); 1979.
[38] Grubb MA, Carskaddan PS. Autostress design of highway bridges phase 3: moment–rotation requirements. AISI project 188, 97-H-045(018-1); 1981.
[39] Kemp A. Interaction of plastic local and lateral buckling. J Struct Eng ASCE 1985;111(10):2181–96.
[40] Schilling CG. Moment–rotation tests of steel bridge girders. ASCE J Struc Eng 1988;114:134–49.
[41] Schilling CG. Moment–rotation tests of steel girders with ultracompact flanges. Proc. of 1990 Annual Technical Session, Stability of Bridges, Structural Stability Research Council. St. Louis, Missouri; 1990.
[42] Wargsjö A. Plastisk Rotationskapacitet hos Svetsade Stalbalkar. Licentiate thesis, 1991:15LDivision of steel structures. Sweden: Lulea University of Technology; 1991 . ISSN 0280-8242, (in Swedish).
[43] Dahl W, Langenberg P, Sedlacek G, Spangemacher R. Elastisch-Plastisches Verhalten von Stahlkonstruktionen Anfoderungen und Werkstoffkennwerte. Doc.-Nr. 7210-Sa/118(91-F6.05). Aachen, Germany: Rheinisch-Westfalischen Technischen Hochshule; 1992.
[44] Boeraeve P, Lognard B. Elasto-plastic behaviour of steel frame works. J Constr Steel Res 1993;27:3–21.
[45] Suzuki T, Ogawa T, Ikaraski K. A study on local buckling behaviour of hybrid beams. Thin-Walled Struct 1994;19:337–51.
[46] Landolfo R, D'Aniello M, Brescia M, Tortorelli S. Rotation capacity and classification criteria of steel beams. The development of innovative approaches for the design of steel–concrete structural systems — the line 5 of the ReLUIS-DPC 2005–2008 Project. Doppiavoce, Napoli: 37–88; 2011.
[47] Zhou F, Young B. Tests of cold-formed stainless steel tubular flexural members. Thin-Walled Struct 2005;43:1325–37.
[48] CEN (European Communities for Standardization). EN 1993-1-1Eurocode 3: design of steel structures—part 1: general rules and rules for buildings; 2005.